Materials Letters 178 (2016) 87–90

Contents lists available at ScienceDirect

Materials Letters

journal homepage: www.elsevier.com/locate/matlet

Microstructure and Luminescence characteristics of self-doped nano-$Mn_3B_7O_{13}Cl$ crystal

Sang Xiong [a], Dong Liang [b], Lin Cao [a,*], Jianlin Sun [a]

[a] School of Materials Science and Engineering, University of Science and Technology Beijing, Beijing 100083, PR China
[b] Boe Technology Group Co., Ltd., Beijing 100010, PR China

ARTICLE INFO

Article history:
Received 25 January 2016
Received in revised form
19 April 2016
Accepted 24 April 2016
Available online 26 April 2016

Keywords:
Nanoparticles
$Mn_3B_7O_{13}Cl$ crystal
Sol–gel preparation
X-ray techniques
Red shift

ABSTRACT

$Mn_3B_7O_{13}Cl$ nanocrystals were firstly prepared by sol-gel process. X-ray diffraction (XRD) and transmission electron microscope (TEM) were utilized to characterize the structure, shape, size of the obtained products. Microstructure and luminescence characteristics of $Mn_3B_7O_{13}Cl$ were discussed. The results show that $Mn_3B_7O_{13}Cl$ nanocrystals can be obtained after xerogel was roasted at 550 °C, the nanocrystals are uniform and the average crystal size is about 50 nm. Two luminescence channels can be observed in $Mn_3B_7O_{13}Cl$ nanocrystal. Luminescence around green wave band (511–541 nm) and red wave band (686–731 nm) are the emission of Mn^{2+} which occupies the center of tetragonal coordination and octahedral coordination, respectively. Both of them are assigned to the transition from $^4T_1$ (G) to $^6A_1$(S) of Mn^{2+}.

1. Introduction

In 1957, chambersite ($Mn_3B_7O_{13}Cl$) was firstly found in the recovered bittern of an oil well in American. Then, the basic chemical constitution, crystal structure, form and physical features were studied, and it is named as “chambersite” by the place of origin in 1962. After that, the mineral was found in Mexico and Louisiana, while none of these can form a level of ore deposit. In 1971, a unique mineral deposit was found in Tianjin of China. So far, this is the only mineral deposit in the word.

In 1975, В.Ф.Белов [1] determined the basic structure of chambersite is B-O skeleton with the method of γ-resonance vibration. Then, its chemical constitution ($Mn_3B_7O_{13}Cl$), crystal structure (trimetric system), morphology physical properties (xenomorphic particle, colorless and transparent, high positive apophasis, notable rough surface, no cleavage, a greyish-white to yellow interference color) was preliminarily studied by Russian researchers. In 1983, professor Yishan Zeng of Beijing university synthesized chambersite by the system of $MnCl_2$-$NaB(OH)_4 \cdot H_2O$ with the temperature of 100 °C and 200 °C [2]. With the extremely luxuriant structure and excellent properties, borate was widely used in the field of laser materials, luminescent materials, dielectric materials, nuclear protect materials and so on [3–4], so it caught lots of attentions. However, the research about this unique and rare structure of macromolecule was comparatively less. Because China is the only country that has a level of ore deposit of chambersite, exploiting and making use of chambersite is of a significant importance.

Sol-gel method is one of wet chemistry methods, as its high uniformity, high purity, low sintering temperature (lower 400–500 °C than traditional method), easier to control, which can be widely used to synthesis nano-materials [5–6]. $MnCl_2$ and $Na_2B_4O_7$ work as precursor were used to synthesis nano-$Mn_3B_7O_{13}Cl$ and its characteristics of microstructure and luminescence have been discussed in this research.

2. Experiments and methods

The $Mn_3B_7O_{13}Cl$ crystal used in this work were prepared by sol–gel technology using starting materials of $MnCl_2 \cdot 2H_2O$ and $Na_2B_4O_7 \cdot 10H_2O$.

Fig. 1 shows schematic representation of $Mn_3B_7O_{13}Cl$ nanocrystal. Keeping heating and magnetic stirring at 110 °C, the xerogel could be obtained, and then sintered at 550 °C for 240 min in air atmosphere. The achieved crystals were milled, washed, filtered, and milled. Hoary crystals were achieved finally.

The crystalline phases were identified by X-ray diffraction (XRD) analysis on a Philips X'Pert diffractometer with the Cu Kα radiation. By using MDI Jade software, the crystalline phases have been analyzed and the crystal size has been calculated with

* Corresponding author.
E-mail address: ld_fans@126.com (L. Cao).

http://dx.doi.org/10.1016/j.matlet.2016.04.196
0167-577X/

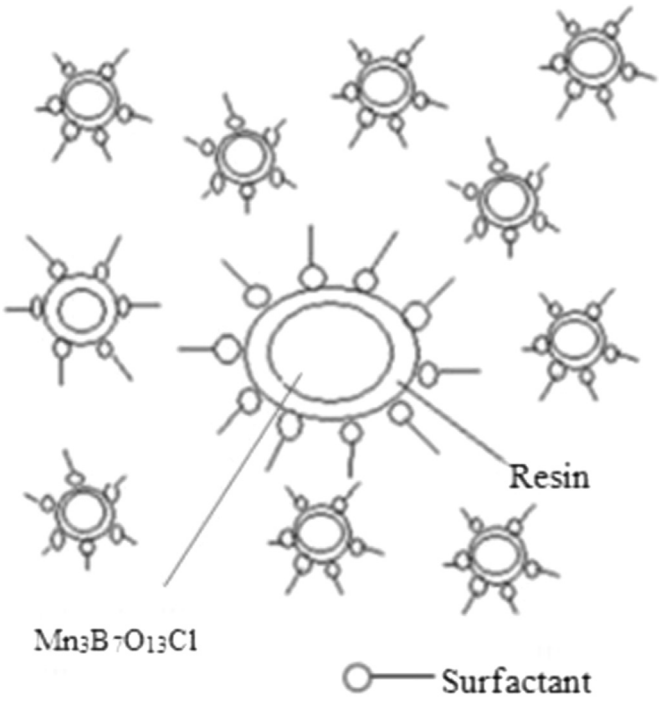

Fig. 1. schematic representation of the formation of Mn3B7O13Cl nanoparticles.

Scherrer formula:

$$\text{Size}=\frac{K\lambda}{FW(S)\cos(\theta)}$$

where Size, K, λ, FW(S), and θ stand for the crystal size, Scherrer constant, full width at half maximum and diffraction angle.

3. Results and discussion

The XRD patterns of $Mn_3B_7O_{13}Cl$ crystals have been measured and are shown as Fig. 2(a). All diffraction peak positions and relative intensity can match the standard PDF card of $Mn_3B_7O_{13}Cl$ well with cell constants of a=8.68 Å, b=8.68 Å, c=12.26 Å and α=β=γ=90°. The crystal belongs to orthorhombic group (Pca21) with four formula units per unit cell. The average size of crystal gain is 48.4 nm calculated by Scherrer formula. Here we must discuss two questions: (1) where does Mn^{2+} ion occupy, and (2) how do the Mn^{2+} ions affect luminescence spectra. Calculation and simulation analysis of HREM images and luminescence spectra provide the answers as we discussed in the following paragraphs. Microstructure features of the samples were investigated using TEM images, as shown in Fig. 2(b) the achieved particles of $Mn_3B_7O_{13}Cl$ form the shape of spherical and have a uniform dispersion. The average particle size is about 50 nm which agree with the calculation result of Scherrer formula.

Fig. 3(a) shows the HREM image of $Mn_3B_7O_{13}Cl$ nanocrystal, in which a number of atomic vacancies are obviously existed. Demarcate and calculate the selected area, the atomic filter image would be achieved, as Fig. 3(b) shows. The real interplanar spacing of $(\bar{1}11)$ is 0.5716 nm. Calibration of each crystal plane, calibration results as shown Fig. 3(c), which can be obtained by Fourier transformation from Fig. 3(b). After calculating by parallelogram law, the result is consistent with the actual calibration and comparing with the data of standard PDF card, the results coincide with each other very well. To distinguish the elements and confirm the phase relation of each atom in HREM image, the simulation image and framework model have been made by EMS software and are show in Fig. 4. In structure of borate, Boron and oxygen ions always form as the structure of BO_3 flat triangle and BO_4 tetrahedral groups [7], while in $Mn_3B_7O_{13}Cl$ crystals, a boron ion is tetrahedral coordinated by four oxygen ions with full T_d symmetry and each Mn^{2+} ion surrounded by four O^{2-} ions and two Cl^- ions has a octahedral coordination. Because of the unique macromolecular structure, bonds between boron ions and oxygen ions are stretched [8], and the tetrahedral center space is expanded, the energy barrier which B^{2+} ions escape from the center of tetrahedron is reduced. As a result, in the crystal of $Mn_3B_7O_{13}Cl$, it is easier to generate vacancies of B^{3+}. Comparing with HREM image, we can easily find that most of the atomic vacancies are due to the absence of B^{3+} centers, i.e. A-site in Fig. 3(a).

The emission spectra of $Mn_3B_7O_{13}Cl$ excited at 450 nm, 460 nm, 470 nm, 480 nm, 490 nm have been measured and are shown in Fig. 5. Note two concentrations of these spectra. Firstly, it is interesting to point out that each spectrum excited at different wavelength has two emission peaks, the shorter wavelength emission (511–541 nm) and the longer wavelength emission (686–731 nm). The green emission (511–541 nm) and red emission (686–731 nm) assigned to the *d-d* transition and spin-forbidden transitions associated with Mn^{2+} ions occupying different sites of the crystal.

The emission of Mn^{2+} are due to the transition of $^4T_1$ (G)–$^6A_1$(S) [9–12], while, ligand field strength has a greater influence on the energy level of $^4T_1$ (G) than $^4A_1$ (G) and ^4E (G). So, in Fig. 3, many atomic defects of B^{3+} ions are observed in the crystal, which benefit the shorter wavelength emission of Mn^{2+} ions embedding in tetragonal field exhibits green luminescence from the $^4T_1$ (G)–$^6A_1$(S) transition. And most of the Mn^{2+} ions occupy

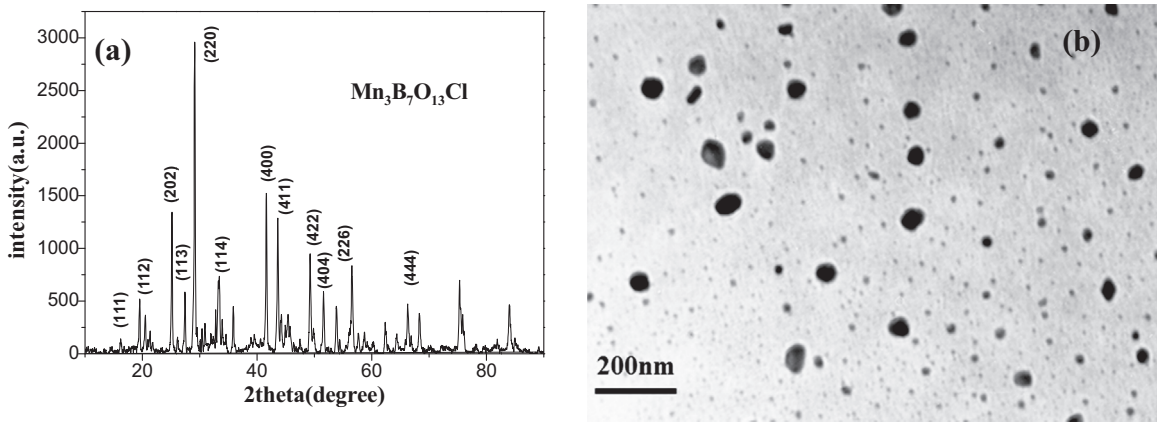

Fig. 2. XRD patterns of $Mn_3B_7O_{13}Cl$ crystals (a) and TEM images of $Mn_3B_7O_{13}Cl$ nanoparticles (b).